Mapping the fluorescence yield on turbid media

Jianan Y. Qu,[a] Zhijian Huang, and Jianwen Hua
Department of Electrical and Electronic Engineering, Hong Kong University of Science and Technology, Clear Water Bay, Kowloon, Hong Kong, People's Republic of China

(Received 4 August 1999; accepted for publication 20 December 1999)

In this letter, we introduce a combined polarization and fluorescence imaging technique for the measurement of fluorescence yield on the surface of turbid media. We use the cross-polarization method to reject the specular reflection and enhance the diffusive backscattering from the turbid media. It has been found that the ratio image of fluorescence versus cross-polarized reflection is not sensitive to the geometry of fluorescence excitation and illumination, and provides a map of fluorescence yield on the surface of imaged subject. The technique reported in this letter may potentially solve the problem for imaging of early cancers which usually start from the superficial layer of tissue and have the fluorescence yield lower than surrounding normal tissue. © *2000 American Institute of Physics.* [S0003-6951(00)00808-1]

It has been proved that the laser-induced fluorescence (LIF) of endogenous fluorophores can be used to diagnose the diseased tissue, especially the early stage cancers.[1] Extensive investigations reveal that the fluorescence yield of early lesions are almost always lower than that of the surrounding normal tissues.[1–6] In principle, the contrast in fluorescence yield can discriminate the lesion from the surrounding normal tissue. Unfortunately, the conventional LIF imaging techniques cannot map the fluorescence yield because of the geometrical effects on measurement of fluorescence power, such as varying separation of the source-sample detector and incident/emission angles over the surface of imaged subject. There have been several publications on different approaches to reduce the geometrical effects. The ratio of fluorescence versus reflection of excitation was demonstrated not sensitive to variations in distance, angle and the excitation power in a nonimaging approach.[5] However, the specular reflection from the surface produced the artifacts and false positives. In Ref. 6, a method combining ultrasound and fluorescence spectroscopy was used to compensate for the detector-sample separation in a special geometry. In a digital approach, a low-pass filter based image processing method was reported to eliminate the geometrical effects under several restrict conditions.[4] In this letter, we introduce a new imaging technique which maps the fluorescence yield on the surface of the turbid media of optical properties in the range of typical human tissue.

The measurable of a typical LIF imaging system are fluorescence and reflection of excitation. We conducted a theoretical investigation on the fluorescence and diffusive reflectance from a homogeneous turbid medium. The method of the Monte Carlo modeling used in this study was discussed in Refs. 3 and 7. The absorption coefficient (μ_a), scattering coefficient (μ_s), and anisotropic factor (g) of the medium were chosen to be in the range of typical human tissues.[8] The excitation/collection geometry and the modeling results are shown in Fig. 1. It is an important finding that the backscattering of excitation has almost the same distribution as fluorescence when the emission angle is not greater than 70°. The geometrical effects on the fluorescence measurement can be effectively corrected by normalizing the fluorescence to the reflectance emitted from the same site. Although the geometry with a fixed illumination perpendicular to the sample surface used in the modeling is not appropriate for many applications, the result seems encouraging. Unfortunately, the computation time and data space will increase tremendously when the Monte Carlo method is used to study the fluorescence and diffusive reflectance in a practical geometry such as an endoscopic imaging system.[7] The experimental investigation is more efficient.

The reflection recorded by a typical LIF imaging system consists of three components: specular reflection, near-diffusive backscattering,[9] and diffusive backscattering. In which, the specular reflection does not carry any information of light propagation inside tissue and must be removed to prevent the artifacts.[5] It is well known that the polarization state of light changes when the scattering event occurs. The multiple scattering process in the turbid media, which yields the diffusive reflectance, randomizes the polarization state of a polarized illumination. In contrast, the specular reflection keeps the original polarization state of excitation light. A cross-polarization imaging system can reject the specular reflection and enhance the diffusive components in total reflectance.[10,11] Experimentally, we illuminated the tissue-

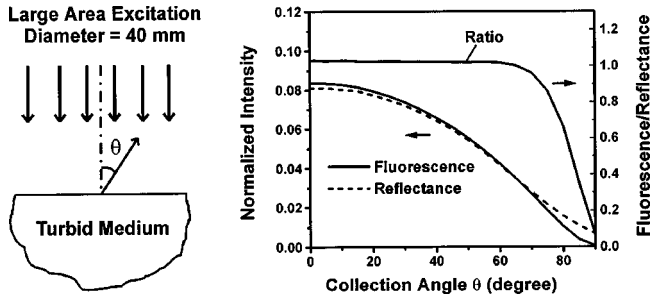

FIG. 1. Left: Illumination and collection geometry. Right: Monte Carlo modeling results. Optical properties of turbid medium at wavelength of excitation: $\mu_a = 3.3\ \text{cm}^{-1}$, $\mu_s = 95\ \text{cm}^{-1}$, and $g = 0.9$; at wavelength of fluorescence emission: $\mu_a = 1.6\ \text{cm}^{-1}$, $\mu_s = 75\ \text{cm}^{-1}$, and $g = 0.87$.

[a]Electronic mail: eequ@ust.hk

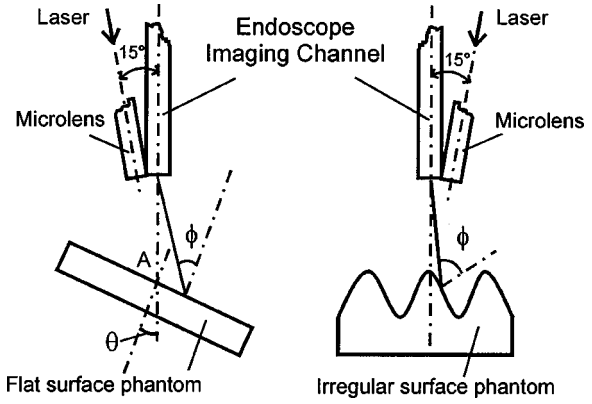

FIG. 2. Schematic diagram of the experimental setup.

like sample (turbid medium) with a linearly polarized laser of wavelength at 457 and output of 200 mW as shown in Fig. 2. The fluorescence and reflection were collected by a commercial endoscope. The images were recorded by an 8-bit charge-coupled device (CCD) camera and grabbed by a frame grabber at rate of 25 frames per second. The holder with a long-pass filter of cut-off wavelength at 470 nm and a polarizer of the polarization axis perpendicular to excitation laser was placed in front of CCD and allowed for easily recording the fluorescence or cross-polarized image. The distance from the tip of endoscope to sample surface was about 10 mm. The imaged area on the sample surface was about 10×10 mm at $\theta=0°$ and smaller than illuminated area. To improve the signal-to-noise ratio, the fluorescence image is formed by taking average of 16 image frames. A ratio image was formed by normalizing the fluorescence image to the cross-polarized reflection image recorded from the same area on the sample surface. The specular reflection was almost completely rejected by the imaging system with extinction ratio ~100:1.

The tissue-simulating turbid media were made of gelatin with 20% solids dissolved in boiling deionized water, polystyrene spheres of 0.55 μm in diameter, fluorescent dye mixture and dominantly absorbing blood. The method to prepare the gel-based solid phantom is well documented.[12,13] The scattering coefficients, controlled by the concentration of the polystyrene microsphere, and g factor are calculated by Mie theory.[13,14] The g factor of 0.55 μm polystyrene microsphere in gel-water matrix is from 0.90 to 0.82 in the wavelength range of 450–700 nm. The scattering coefficients of the samples with microsphere concentrations at 0.25%, 0.35%, and 0.5% weight-by-weight in the same wavelength range vary from 95 to 39, 133 to 55, and 190 to 78 cm^{-1}, respectively. The absorption of the tissue phantoms were determined by the concentration of the blood. We set the content of blood with hematocrit 0.51 of three groups of tissue phantoms to 2.5%, 5%, and 7.5% volume-by-volume, respectively. The optical properties of all samples are in the typical range of human tissue.[8] We used the mixture of highly fluorescent dyes of green and red STABILO BOSS highlighters to simulate the endogeneous fluorophores in tissue. The fluorescence of the dye mixture covers the same spectral region as *in vivo* measured tissue autofluorescence. Table I summarizes the compositions of all the homogeneous samples.

The fluorescence and cross-polarized images were collected from all samples of flat surface at $\theta=0°-6°$ with increments of 15° shown in Fig. 2. We did not perform the measurement for $\theta>60°$ due to the limited dynamic range and sensitivity of 8-bit CCD camera and the aberration of the imaging system. The images of irregular surface sample were collected at $\theta=0°$. The width and the depth of the grooves on the surface are about 8 and 5 mm, respectively. For a fair comparison, the mean gray levels of all the raw fluorescence images and ratio images have been adjusted to 128, half of the full gray levels of an 8-bit image. The typical results are shown in Fig. 3. As can be seen, the gray levels of raw fluorescence images vary in a wide range, while the ratio images are uniform. It was found that the standard deviations of gray levels for the raw fluorescence images recorded from homogeneous samples vary from 24 to 41 at $\theta=0°-60°$. In contrast, the standard deviations of ratio images vary from 1.8 to 5, much smaller than the raw fluorescence images. The geometrical effects have been corrected to a great extent in ratio image. The second experiment was designed to demonstrate that a slight variation in the fluorescence yield of tissue could be identified by this ratio imaging technique. The structure of the fluorescence yield contrast sample with the uniform optical properties same as the irregular surface sample is shown in Fig. 4. The fluorescence yield of simulating lesions was set to about 80% of that of surrounding samples. Two holes were made to create the interference for identifying the simulating lesions. The raw fluorescence and ratio images of the fluorescence yield contrast sample are shown in Fig. 4. In the raw fluorescence image, it is not possible to distinguish the lesions from the artifacts created by two holes. However, the contrast in fluorescence yield between simulating lesions and surrounding sample has been

TABLE I. Compositions of the homogeneous phantoms with flat surface.

Flat surface	Blood content	Concentration of scatterer
1	2.5%	0.25%
2	5.0%	0.25%
3	7.5%	0.25%
4	2.5%	0.5%
5	5.0%	0.5%
6	7.5%	0.5%
Irregular surface	5%	0.35%

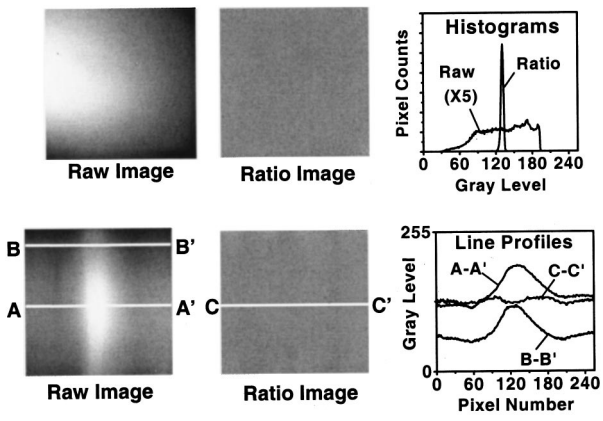

FIG. 3. Above: raw fluorescence image and ratio image recorded from sample No. 4 at $\theta=30°$ and histogram analysis. Below: raw fluorescence image and ratio image of irregular surface sample and line profile analysis.

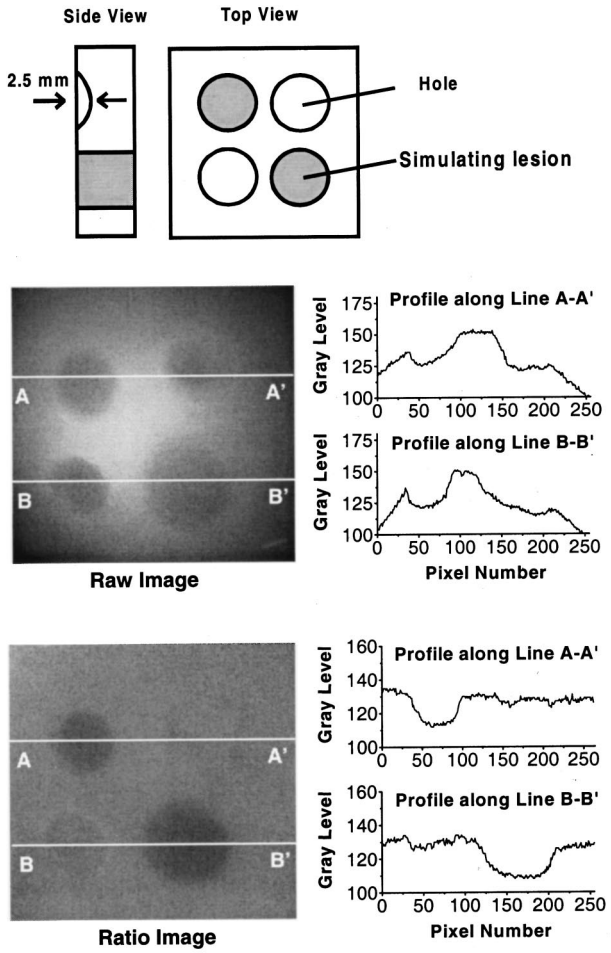

FIG. 4. Top: structure of the fluorescence yield contrast sample; middle: raw fluorescence image and its line profile analysis; bottom: ratio image and its line profile analysis.

clearly recovered, and the artifacts caused by the holes were almost completely eliminated in the ratio image.

It has been found that the ratio value of fluorescence versus cross-polarized reflection was slightly dependent on the excitation and collection angle ϕ shown in Fig. 2, but not sensitive to the polarization orientation of excitation and optical properties of samples. The averaged ϕ dependence of the ratio based on all measurements is shown in Fig. 5. The ratio value at $\theta > 70°$ becomes not reliable because of the poor performance of the imaging system at $\theta > 60°$. The maximal variation of ratio in the range of angle ϕ from 0° to 70° is less than 7%, which is much smaller than the contrast in fluorescence yield between early lesion and normal tissue on most of clinically investigated organ sites.[1–6] The theoretical and experimental investigations indicate that the correction of the geometrical effects is due to the similar characteristics of fluorescence and cross-polarized reflection. The fluorescence emitted from the isotropic fluorescence sources is diffusive. The cross-polarized reflection is yielded by diffusive and near-diffusive backscattering. The diffusive component in the cross-polarized reflection creates the major contribution to the correction of geometrical effects. The near-diffusive component favors the large angle backscattering in the tissue, a forward-scattering dominated turbid medium.[9] The correction of geometrical effects requires that the diffusive component must be much larger than near diffusive in the cross-polarized reflection. This condition is generally satisfied in scattering dominated turbid media ($\mu_s \gg \mu_a$ and $g \sim 0.9$) such as human tissue.

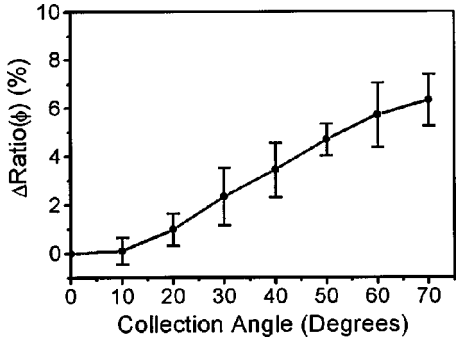

FIG. 5. Relative change of ratio value as the function of excitation and collection angle ϕ, where $\Delta\text{Ratio}(\phi) = [\text{Ratio}(\phi) - \text{Ratio}(0)]/\text{Ratio}(0)$.

[1] G. A. Wagnieres, W. M. Star, and B. C. Wilson, Photochem. Photobiol. **68**, 603 (1998).
[2] N. Ramanujam, M. F. Mitchell, A. Mahadevan, S. Thomsen, E. Silva, and R. Richards-Kortum, Gynecol. Oncol. **52**, 31 (1994).
[3] J. Qu, C. MacAulay, S. Lam, and B. Palcic, Opt. Eng. (Bellingham) **34**, 3334 (1995).
[4] T. D. Wang, J. van Dam, J. M. Crawford, E. A. Preisinger, Y. Wang, and M. S. Feld, Gastroenterology **111**, 1182 (1996).
[5] A. E. Profio, D. R. Doiron, and J. Sarnaik, Med. Phys. **11**, 516 (1984).
[6] S. Warren, K. Pope, Y. Yazdi, A. J. Welch, S. Thomsen, A. L. Johnston, M. J. Davis, and R. Richards-Kortum, IEEE Trans. Biomed. Eng. **42**, 121 (1995).
[7] L. Wang and S. L. Jacques, ''Monte Carlo modeling of light transport in multilayered tissue in standard C,'' University of Texas M. D. Anderson Cancer Center (1992).
[8] W. F. Cheong, S. A. Prahl, and A. J. Welch, IEEE J. Quantum Electron. **QE-26**, 2166 (1990).
[9] L. Wang and S. J. Jacques, Proc. SPIE **1888**, 107 (1993).
[10] S. G. Demos and R. R. Alfano, Appl. Opt. **36**, 150 (1997).
[11] G. D. Lewis, D. L. Jordan, and P. J. Roberts, Appl. Opt. **38**, 3937 (1999).
[12] A. J. Drukin, S. Jaikumar, and R. Richards-Kortum, Appl. Spectrosc. **47**, 2114 (1993).
[13] L. Wang and X. Zhao, Appl. Opt. **36**, 7277 (1997).
[14] M. Kohl, M. Essenpreis, and M. Cope, Phys. Med. Biol. **40**, 1267 (1995).